Korean J. Chem. Eng., **31**(5), 911-917 (2014)
DOI: 10.1007/s11814-013-0297-z

pISSN: 0256-1115
eISSN: 1975-7220

Synthesis and characterization of cross-linked poly(acrylic acid)-poly(styrene-*alt*-maleic anhydride) core-shell microcapsule absorbents for cement mortar

Kiseob Hwang* and Kiryong Ha,†**

*Korea Institute of Industrial Technology, 89, Yangdaegiro-gil, Ipjang-myeon, Seobuk-gu, Cheonan-si, Chungcheongnam-do 331-822, Korea
**Department of Chemical Engineering, Keimyung University, Dalseo, Deagu 704-701, Korea
(*Received 25 July 2013 • accepted 30 December 2013*)

Abstract−We synthesized core-shell microcapsule absorbents with cPAA (cross-linked poly(acrylic acid)) as the core and PSMA (poly(styrene-*alt*-maleic anhydride)) as the shell by precipitation polymerization, where the shell served to delay the absorption of excess water in cement mortars. To control shell thickness, the cPAA-PSMA capsules were synthesized with core monomer mass to shell monomer mass ratios of 1/0.5, 1/1, and 1/1.5. We observed the hydrolysis of the PSMA polymer in a cement-saturated aqueous solution by Fourier transform infrared (FT-IR) spectroscopy. Furthermore, core-shell structures were observed for 1/1 (cPAA-PSMA #3) and 1/1.5 (cPAA-PSMA #4) core/shell monomer mass ratios, whereas no core-shell structures were observed for the 1/0.5 (cPAA-PSMA #2) microcapsules by transmission electron microscopy (TEM).

Keywords: cPAA-PSMA, Hydrolysis Reaction, Core-shell, Microcapsule, Absorbent

INTRODUCTION

When concrete is made, in general, more water is added than the theoretically necessary amount. Although the theoretical amount of water-cement ratio (W/C-ratio) lies between 25-30% (wt./wt.), the W/C-ratio used practically is 50-60%. The purpose of this 25-30% excess of water is to enhance the workability of the concrete [1,2]. Unfortunately, the excess water can cause a decrease in compressive strength, along with an increase in bleeding and shrinkage cracks [2,3]. It can also decrease the concrete's long-term durability by chloride ion permeation, carbonation, and freeze-thaw cycles [4].

Several studies have attempted to address the problems that arise from the excess of water in concrete. One study used a so-called dewatering mold form (DMF) of concrete, which contains many holes on the surface of DMF to drain the excessive water [5]. However, this method drains excess water from the concrete surface contacting DMF only, while the excess water at the top (layer on half) of concrete in DMF cannot be drained out effectively due to the small pressure. For a more complete solution, we have investigated the synthesis of core-shell structured microcapsule absorbents that initially resist the absorption of mixing water (i.e., at zero concrete mixing time) but, after a defined time, start to absorb water in the core as a result of the dissolution of the shell in the alkaline environment of the cement water.

The PSMA is known to be transparent, have high thermal resistance and dimensional stability [6]. When the anhydride groups in PSMA are in contact with alkaline aqueous solution, the anhydride ring hydrolyzes and forms carboxylate salts, resulting in PSMA swelling or dissolution depending on whether the PSMA is cross-linked or not, as shown in Fig. 1 [7,8]. The solubility of PSMA in alkaline aqueous solutions makes it suitable for various applications such as in sizing (gluing to clothes), as binders, and in coatings [9].

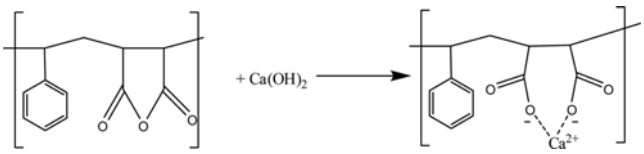

Fig. 1. Hydrolysis and neutralization reaction of PSMA in alkaline aqueous solution.

In this study, we investigated the synthesis of core-shell microcapsule absorbents that contain cPAA as the core and PSMA as the shell. The product was added to cement mortars to absorb excess water after a specified time.

EXPERIMENTAL

1. Materials

We performed precipitation polymerization to make core-shell microcapsule absorbents comprised of a cross-linked PAA core and a non-cross-linked PSMA shell. Toluene (OCI Company Ltd.) was used as solvent, AA (acrylic acid, DuckSan Pure Chemical) was passed through an inhibitor removing column (Aldrich) before use. The cross-linking agent MBA (*N,N′*-methylene bisacrylamide, Acros Organic, 96%), St (styrene, Aldrich), MA (maleic anhydride, Aldrich), and AIBN (2,2′-azobisisobutyronitrile, Daejung) were used without further purification. Portland cement (Ssangyong cement, called "cement") was used as received.

2. Precipitation Polymerization

To synthesize the core of the core-shell microcapsule absorbent, we used AA as the monomer with MBA as a cross-linking agent

†To whom correspondence should be addressed.
E-mail: ryongi@kmu.ac.kr

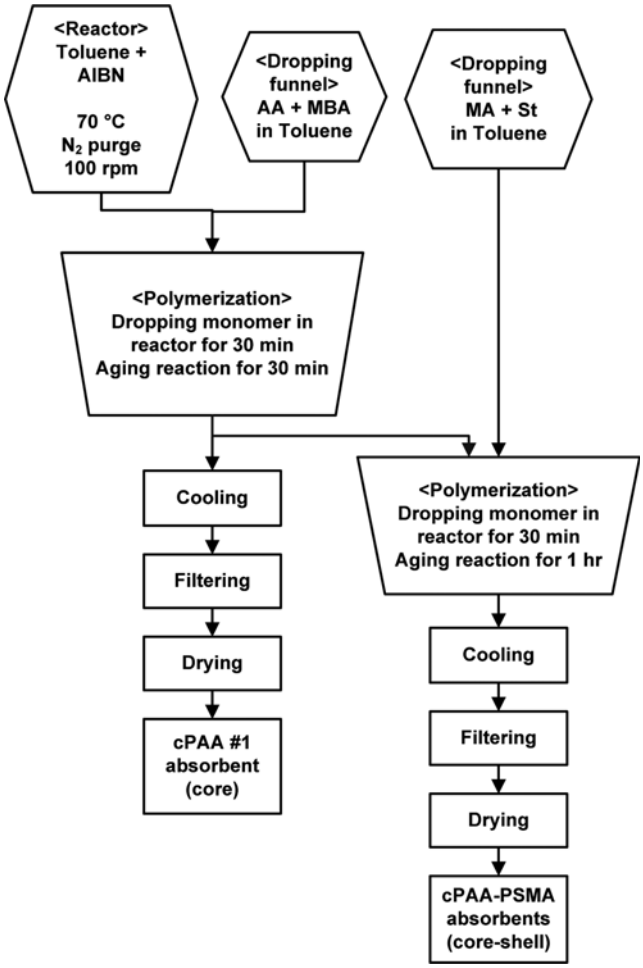

Fig. 2. Flow chart for core and core-shell microcapsule absorbent polymerization.

in toluene to yield cPAA by precipitation polymerization [10,11]. To synthesize the shell part of the absorbent, we copolymerized St and MA to obtain PSMA. We first dissolved an adequate amount of MA in toluene (8.10 g MA/100 ml toluene solution), and added St and radical initiator using a dropping funnel, where the initiator can be organic peroxide or AIBN. Through this method, we obtained an almost perfectly alternating copolymer [9,12,13].

For the complete core-shell microcapsule synthesis procedure, see Fig. 2. A 500-ml glass reaction flask (5-neck 500-ml Pyrex glass reaction flask) was used in the polymerization of cPAA. Toluene (100 mL) and 0.6 g AIBN were added into the bottom reactor, after which it was covered with the reactor head. The reactor was fitted to a condenser, stirrer (WiseStir™, Daihan Scientific Co.), nitrogen inlet tube, and a dropping funnel. The temperature was maintained at 70 °C using a water bath (WB-23, SIBATA). The reactor was purged with N_2 gas, and stirred at 100 rpm to dissolve the AIBN in toluene. Then, 30 g of AA and 0.1 g of MBA were mixed and poured into the dropping funnel and added drop-wise into the reactor over a period of 30 min. Polymerization was then continued for another 30 min [10,11].

When polymerization was completed, the reactor was cooled to room temperature by exchanging the hot water in the water bath with room temperature tap water. The polymerized product in the reactor was filtered through a filter paper, dried at 50 °C in an oven to remove excess toluene, and further dried in a vacuum oven for 24 h. The resulting dried solid was termed cPAA #1.

Table 1. Composition of cPAA-PSMA polymerization

	Polymer	AA	MBA	Toluene
Core	cPAA #1	30 g	0.1 g	100 ml
	Polymer	MA	Styrene	Toluene
Shell	cPAA-PSMA #2	7.4 g	8.1 g	100 ml
	cPAA-PSMA #3	14.7 g	16.2 g	200 ml
	cPAA-PSMA #4	22.1 g	24.3 g	300 ml

The shell of the cPAA-PSMA core-shell microcapsule absorbent was synthesized by using different mass ratios of St and MA monomers to core cPAA #1. Shell polymerization was performed according to the method of Liu, et al. [14]. After dissolving MA and St in toluene, we added the solution into the dropping funnel in the compositions shown in Table 1. This solution was slowly added drop-wise into the cPAA #1 mixture over 30 min and polymerized for an additional hour under the same conditions as the core polymerization.

Upon completion of the shell polymerization, the reactor was cooled to room temperature by exchanging the hot water in the water bath with room temperature tap water. The polymerized product in the reactor was filtered through filter paper, washed three times with toluene, dried at 50 °C in an oven to remove excess toluene, and further dried in a vacuum oven for 24 h (see Fig. 2).

3. Characterization

For FT-IR analysis, the polymers and the dried samples after swelling were mixed with KBr powder to make pellets, and FT-IR transmittance spectra were acquired with an FT-IR spectrometer (Jasco, FT/IR 620, scan range: 4,000 cm^{-1} to 400 cm^{-1}, resolution: 4 cm^{-1}, 100 scans=1 spectrum).

For field emission scanning electron microscope (FE-SEM) analysis, each polymer was diluted three times with toluene, dropped on a slide glass, and dried. Each dried specimen was analyzed after Pt coating by FE-SEM (Hitachi S-4300).

For TEM analysis, each polymer was embedded in epoxy resin (Epon 812 kit, Ted Pella), and cut in 60-nm-thick sledges by an ultramicrotome (MT-X, RMC). The cut sample was placed on a carbon type 200-mesh copper grid. TEM analysis (H-7600, Hitachi) was conducted by controlled contrast without specimen staining [15,16].

Swelling ratios for the synthesized absorbents were measured in a cement-saturated aqueous solution (CSAS) with 0.10 g polymer absorbent in a nylon-screen tea bag (250 mesh). Synthesized absorbents usually form aggregates after drying; therefore, they were crushed to about 1 mm granular by using a pestle and mortar before swelling measurements. CSAS was prepared by adding excess cement to 2,000 ml of D.I. water and stirring with a glass rod for 3 h. The supernatant was used as CSAS.

RESULTS AND DISCUSSION

1. FT-IR Measurements

FT-IR was used in the transmittance mode to identify the pres-

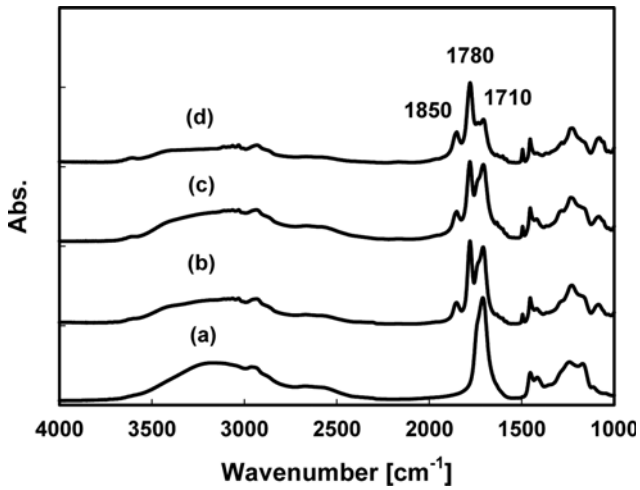

Fig. 3. FT-IR spectra of (a) cPAA, (b) cPAA-PSMA #2, (c) cPAA-PSMA #3, and (d) cPAA-PSMA #4 (before swelling).

ence of the anhydride ring for the synthesized PSMAs as well as to monitor the structural changes in cPAA and cPAA-PSMA samples before and after swelling in CSAS.

FT-IR spectra for cPAA and cPAA-PSMAs before swelling are shown in Fig. 3. For cPAA #1, we observed the -OH stretching vibration at 3,200 cm^{-1}, the -CH_2 asymmetric and symmetric stretching vibrations at 2,924 cm^{-1} and 2,855 cm^{-1}, respectively [17], and the -C=O stretching of the carboxylic acid at 1,710 cm^{-1}. FT-IR spectra of cPAA-PSMA #2, cPAA-PSMA #3, and cPAA-PSMA #4 showed the -OH stretching vibration at 3,200 cm^{-1}, the C-H stretching of the benzene ring from 3,050 to 3,020 cm^{-1}, and aliphatic -CH_2 stretching from 2,960 cm^{-1} to 2,880 cm^{-1}. We also observed the cyclic >C=O anhydride vibrations at 1,850 cm^{-1} and 1,780 cm^{-1} (two peaks [18-20]), as well as -C=O stretching of the carboxylic acid at 1,710 cm^{-1} and the cyclic C-O-C of the anhydride at 1,222 cm^{-1} [21]. These results confirmed the existence of anhydride groups in cPAA-PSMA before swelling, which may undergo hydrolysis in CSAS. An increase in peak intensity at 1,850 cm^{-1} and 1,780 cm^{-1} compared to 1,710 cm^{-1} was also observed with increasing shell core mass ratio for cPAA-PSMA #2, cPAA-PSMA #3, and cPAA-PSMA #4 as shown in Fig. 3.

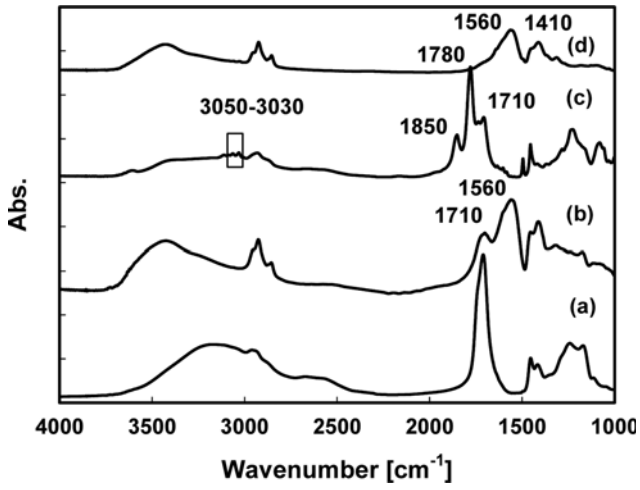

Fig. 4. FT-IR spectra of (a) cPAA before and (b) after alkaline hydrolysis (written H-cPAA), and (c) cPAA-PSMA #4 before and (d) after alkaline hydrolysis (written H-cPAA-PSMA) (4,000-1,000 cm^{-1} region).

To compare the cPAA #1 and cPAA-PSMA #4 before and after 4 h of swelling in CSAS, FT-IR spectra were acquired as shown in Fig. 4. The samples after swelling were dried for seven days at 50 ºC in a drying oven. An intermediate temperature of 50 ºC was used because the temperature of the cement hydration process reaches 50 ºC at center in 1 m×1 m×1 m concrete size [1]. However the temperature of center of cement can reach 30-100 ºC depending on the concrete size due to the release of heat during cement hydration [22].

The FT-IR spectra of the hydrolyzed cPAA #1 (H-cPAA #1) shown in Fig. 4(b) display a weak residual peak at 1,710 cm^{-1}, indicating the C=O stretching vibration of the carboxylic acid. A new peak appeared at 1,560 cm^{-1} as well as several small peaks from 1,450 cm^{-1} to 1,410 cm^{-1}. The peak at 1,560 cm^{-1} stems from the asymmetric stretching vibration of the carboxylate salt, while the peak between 1,450 cm^{-1} to 1,410 cm^{-1} is caused by symmetric stretching of the carboxylate salt [23]. The peaks were thus caused by carboxylate salt formation of the carboxylic acid moieties in c-PAA by the neutralization reaction with the alkaline aqueous solution at pH 12 [18-20,24].

For the cPAA-PSMA #4 after hydrolysis (H-cPAA-PSMA #4) shown in Fig. 4(d), we observed the disappearance of the C-H stretching vibration of the benzene ring in the 3,050-3,030 cm^{-1} region, as well as the disappearance of the cyclic C=O of anhydride stretching vibration at 1,850 cm^{-1} and 1,780 cm^{-1}, and the C=O stretching of carboxylic acid at 1,710 cm^{-1}. New peaks were observed at 1,560 cm^{-1} and at 1,410 cm^{-1}. These spectral changes are caused by hydrolysis of the anhydride moieties of cPAA-PSMA in alkaline CSAS (pH 12) to form the carboxylic acid. After carboxylic acid formation, the neutralized carboxylate is formed by complexation of salt ions such as Ca^{2+} or K^{+} in CSAS. After carboxylate salt formation, the PSMA shell of the cPAA-PSMA absorbents degrades by its dissolution into CSAS. This dissolved PSMA shell part also can act to improve strengths of dried cement mortar [29].

2. SEM Analysis

To measure the particle size of the synthesized cPAA and cPAA-PSMA absorbents with FE-SEM, the samples were diluted in toluene, applied on a glass slide and dried. The FE-SEM image of the core sample cPAA #1 showed the particle size to range between 131-151 nm as shown in Fig. 5(a).

FE-SEM images of cPAA-PSMAs showed the particle size of cPAA-PSMA #2 to range from 129 to 217 nm, while that of cPAA-PSMA #3 and cPAA-PSMA #4 ranged from 187 to 250 nm and 244 to 292 nm, as shown in Fig. 5(b), 5(c) and 5(d), respectively. The FE-SEM results thus support the hypothesis that the particle size of the synthesized absorbent increases with an increase in the amount of shell monomer used (see Table 1).

In this experiment, since the conversion of monomer to polymer is over 95% (as concluded from weight measurements after polymerization), we tried to calculate the radius of absorbent particles from the weights of the monomers used for polymerization by using the formula for the volume of a sphere: $V=4/3\cdot\pi r^3$, where V is the volume of absorbents and r is the radius of the absorbent particle.

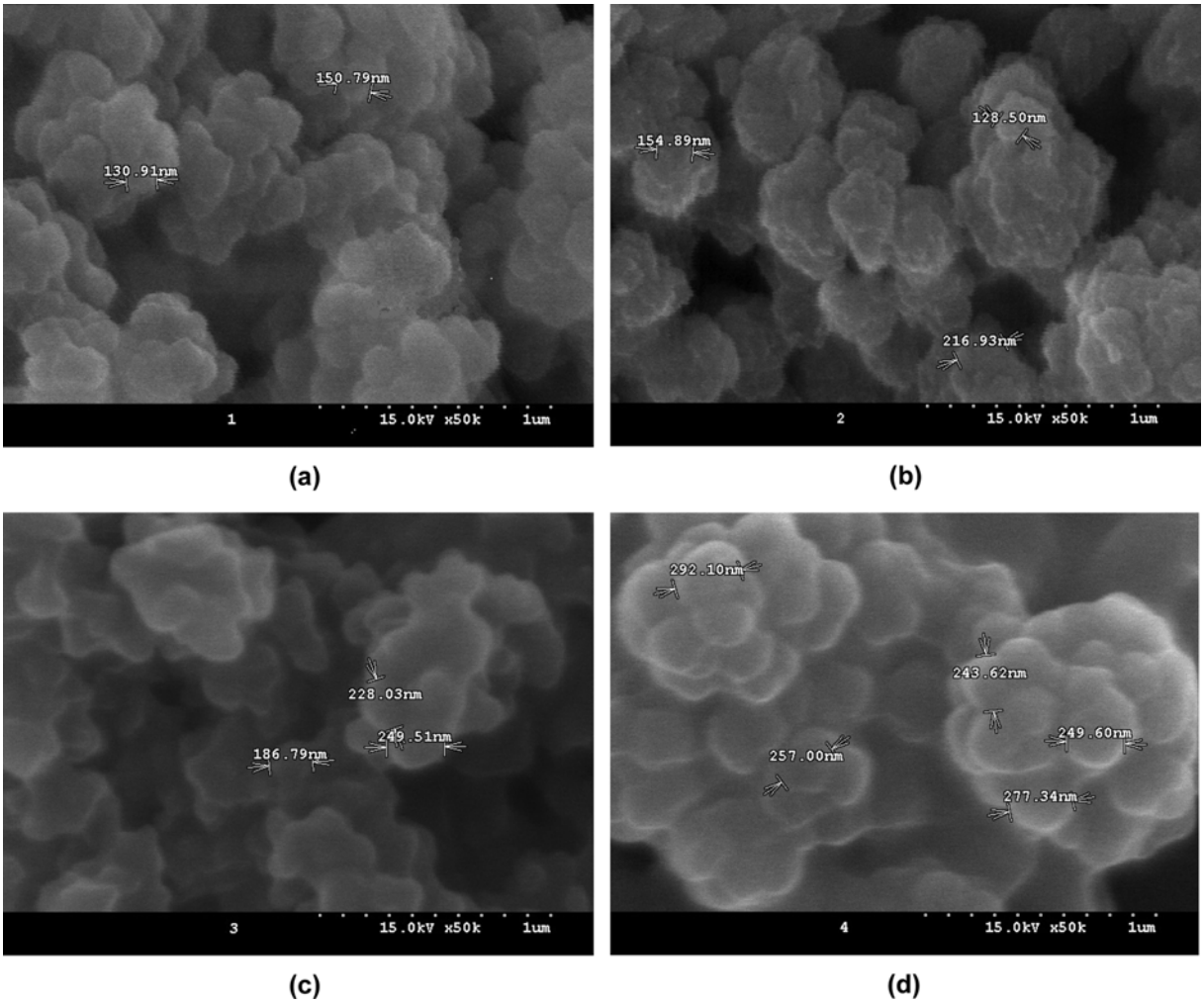

Fig. 5. FE-SEM images of (a) cPAA #1, (b) cPAA-PSMA #2, (c) cPAA-PSMA #3, and (d) cPAA-PSMA #4.

If the density of absorbent polymer is the same as that of the monomer, the calculated radii of cPAA-PSMA #2, cPAA-PSMA #3, and cPAA-PSMA #4 are 1.14, 1.25, and 1.36 times that of cPAA #1, respectively. The radii observed by FE-SEM of cPAA-PSMA #2, cPAA-PSMA #3, and cPAA-PSMA #4 were 1.23, 1.55, and 1.93 times that of cPAA #1, which is slightly larger than the calculated results.

3. TEM Analysis

To investigate the morphology of the synthesized cPAA-PSMA #2, cPAA-PSMA #3 and cPAA-PSMA #4, we conducted TEM analysis as shown in Fig. 6. The TEM images were acquired by controlling the contrast without staining.

As shown in Fig. 6(a), cPAA-PSMA #2 displays very thin or no shell formation at all due to the small amount of shell monomer added compared to the amount of core monomer. For the TEM image of cPAA-PSMA #3 (Fig. 6(b)), core-shell formation was observed, where the bright region in the center of the particle is the cPAA core, while the dark region surrounding the bright region corresponds to the PSMA shell. A similar observation was made for cPAA-PSMA #4 (Fig. 6(c)), which also showed complete core-shell formation.

4. Swelling Ratio Measurements

Swelling ratio measurements for cPAA and cPAA-PSMAs were performed by the tea bag method using 250-mesh nylon screens over a time range of 0 to 1,440 min as shown in Fig. 7. The swelling ratios from 0 min to 60 min are shown separately to indicate the stage where the swelling ratio increases more clearly as shown in Fig. 7(b). The swelling ratios for absorbents were calculated by the equation $Q=(W_2-W_1)/W_1$, where Q is the swelling ratio, W_1 is the weight of dried absorbent before swelling, and W_2 is the weight of the swelled absorbent [24-28]. As is clear from the figure, the swelling ratios for cPAA #1 continuously increases, swelling to 100 times of the initial value after 240 min, and to 110 times of the initial value after 1,440 min. For cPAA-PSMA #2, swelling ratios were 86 after 240 min and 99 after 1,440 min. Since the shell monomer mass to core monomer mass ratio was too low to form a sufficiently thick shell, cPAA-PSMA #2 presumably formed an incomplete shell.

For cPAA-PSMA #3, swelling ratios were 32 after 30 min and decreased to 30 after 60 min. They gradually increased again to reach 59 after 1,440 min. Swelling ratios for cPAA-PSMA #4 were 32 after 30 min, and decreased to 29 after 60 min. They started to increase again to reach 52 after 1,440 min. The swelling ratios for cPAA-PSMA #3 and #4 increased until 30 min, respectively, after which they actually showed a decrease until 60 min. This phenomenon appears to be caused by the fact that hydrolysis of the PSMA

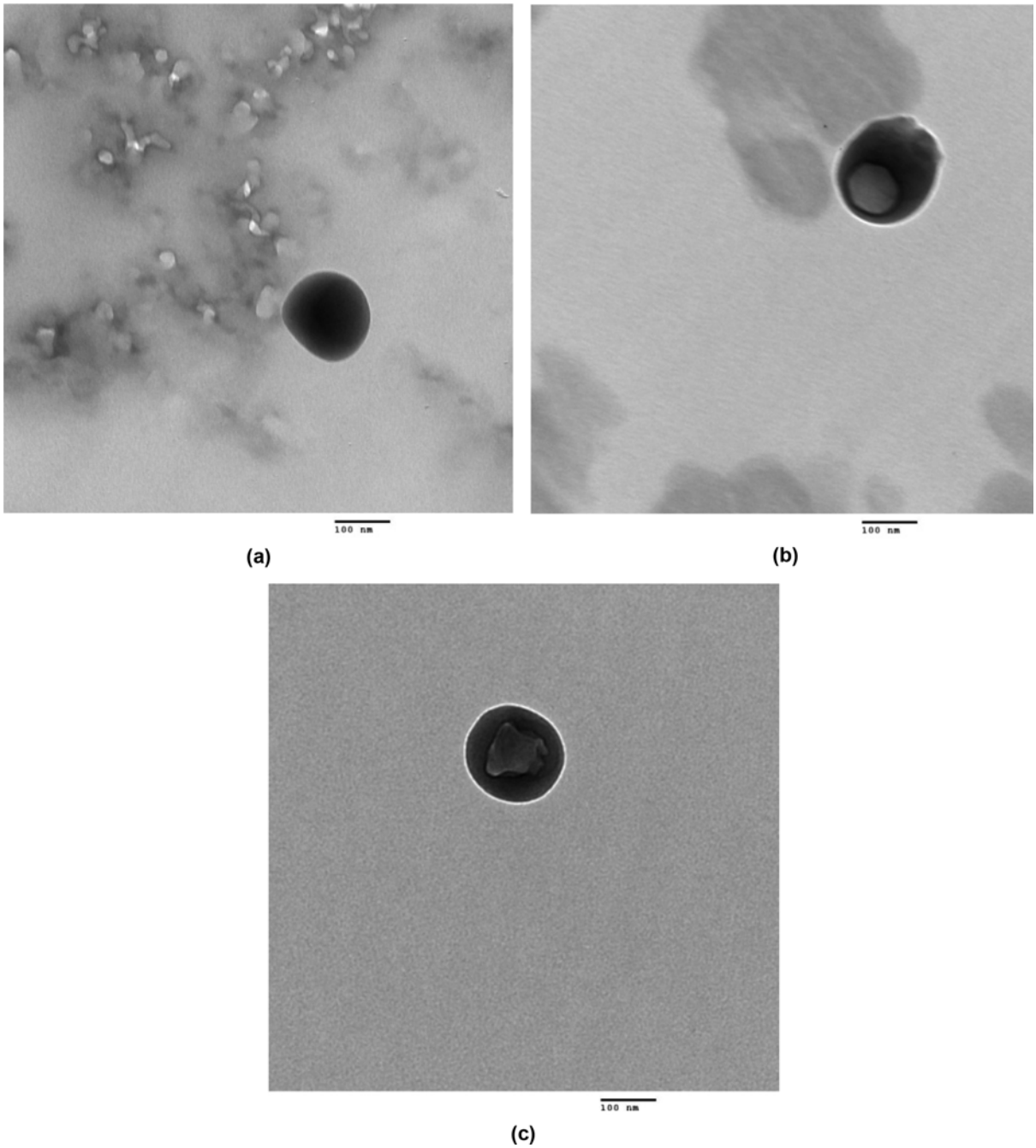

Fig. 6. TEM images of (a) cPAA-PSMA #2, (b) cPAA-PSMA #3, and (c) cPAA-PSMA #4.

shell in CSAS at pH 12 and its swelling and dissolution in the CSAS is a two-stage process. In the first step, the partly hydrolyzed shell absorbs water and swells. In the second step, the swelled hydrolyzed PSMA shell dissolves in CSAS. CPAA-PSMA #3 and #4 showed lower swelling ratios compared to #1 and #2, because of the smaller amounts of core cPAA, which only can absorb excess water once the shell PSMA dissolves into CSAS.

Also, to compare the swelling ratios of synthesized absorbents in DI water and in CSAS, we measured swelling ratios cPAA #1 and cPAA-PSMA #4 in DI water as shown in Fig. 8. As shown in Fig. 8, the swelling ratio of cPAA #1 increases to 200 after 90 min and maintains its value of 200 until 195 min. In contrast, the swelling ratio of cPAA-PSMA #4 increases to 10 after 20 min and maintains its value of 10 until 195 min.

The swelling ratios of cPAA #1 in the CSAS and the DI water are very different due to existence of Ca^{2+} ions in CSAS. The swelling ratio of cPAA # 1 in CSAS showed lower value than that in DI water, because Ca^{2+} ions in CSAS can react with two COO^- ions of cPAA to form ionic crosslink [29], which inhibits swelling of the cPAA. But the swelling ratio of cPAA-PSMA #4 in CSAS showed higher value than in DI water, because Ca^{2+} ions in CSAS can hydrolyze MA of PSMA, and hydrolyzed PSMA part will be dissolved in CSAS. After dissolution of PSMA part, cPAA part in cPAA-PSMA #4 can start to absorb water. But PSMA part of cPAA-PSMA #4

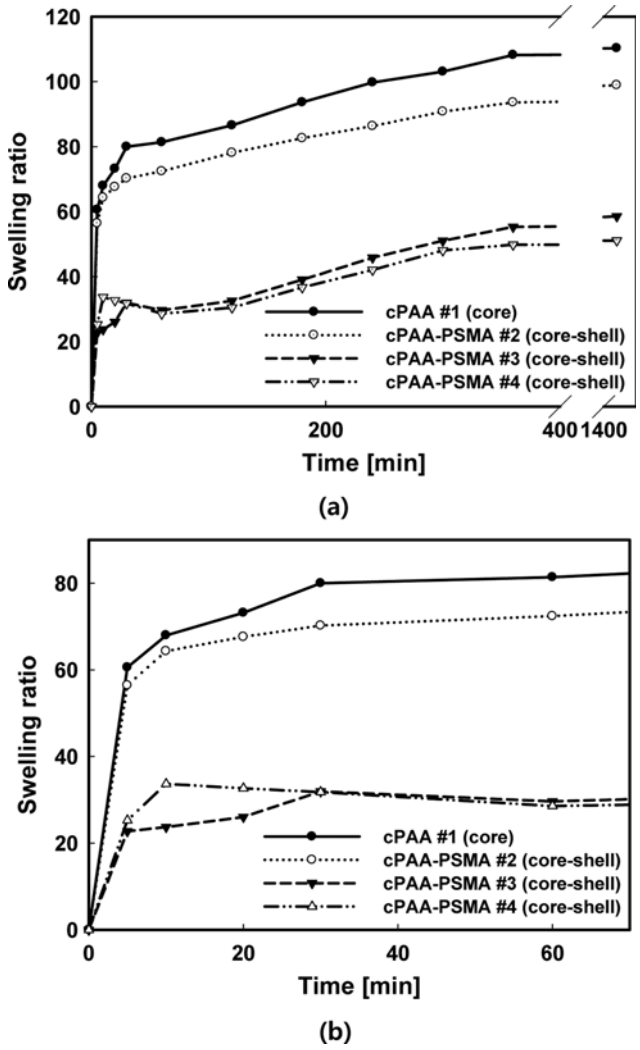

Fig. 7. Swelling ratios for cPAA and cPAA-PSMA series over (a) 0-1,440 min region and (b) expanded in 0-60 min region in cement-saturated aqueous solution.

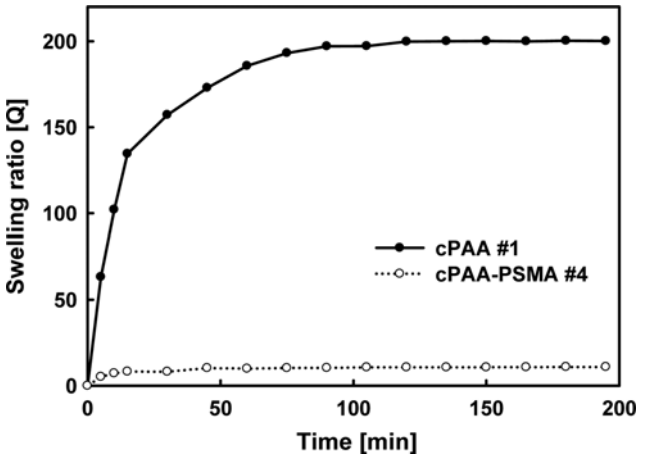

Fig. 8. Swelling ratios for cPAA#1 and cPAA-PSMA#4 in deionized water.

in DI water could not be hydrolyzed; therefore, this PSMA shell part surrounding cPAA remained in DI water, thu, hindering access of water to cPAA part of cPAA-PSMA #4.

Generally, the pore size of concrete made of Portland cement is about 1,000 nm diameter on average [30]. If the absorbents maintain a spherical shape after swelling, the volume of the absorbent can be calculated by using $V=(4\pi r^3)/3$. The particle sizes of swollen cPAA #1, cPAA-PSMA #2, cPAA-PSMA #3 and cPAA-PSMA #4 absorbents in CSAS, which are calculated from the swelling ratios of 1,440 min in CSAS, are 622-718 nm, 592-1,000 nm, 724-970 nm and 930-1,090 nm, respectively. Therefore, the swollen particles can fit in the pore of concrete, not causing any adverse effects on the mechanical properties of concrete.

CONCLUSIONS

We synthesized several different core-shell microcapsule absorbents to preserve the working time of concrete while absorbing excess water thereafter. These core-shell structure microcapsule absorbents were synthesized by precipitation polymerization and contained cPAA as the core material and PSMA as the shell material. The PSMA shell will dissolve or swell by the hydrolysis of anhydride groups in alkaline aqueous solution, depending on whether the shell is cross-linked.

The presence of anhydride groups was identified in cPAA-PSMA absorbents before swelling by FT-IR measurement. After swelling in CSAS due to the hydrolysis and neutralization reaction of the PSMA shell of cPAA-PSMA, the anhydride peaks disappeared and new peaks were observed, stemming from the asymmetric and symmetric stretching vibration of the carboxylate salts.

FE-SEM analysis indicated an increase in particle diameter with an increase of added shell forming monomers. Using TEM analysis, a well-defined core-shell structure was observed for cPAA-PSMA # 3 and cPAA-PSMA # 4 absorbents.

Finally, the swelling ratios for cPAA #1 in CSAS showed a continuous increase with time to reach 110 times of the initial value, after 1,440 min experiment time. In contrast, the swelling ratios for cPAA-PSMA #4 in CSAS showed an increase after 30 min and a decrease from 30 min to 60 min. After 60 min, the ratio increased again to reach 52 after 1,440 min.

The W/C-ratio used is practically 50-60%, even though the theoretical amount of W/C-ratio lies between 25-30% (wt./wt.). The synthesized microcapsule absorbents (cPAA-PSMA #3 and #4) showed swelling ratios of 59 and 52, respectively. Therefore, we may use about 0.5% of synthesized microcapsule absorbents for cement weight to absorb excess water in cement mortar.

REFERENCES

1. D. A. Williams, A. W. Saak and H. M. Jennings, *Cement Concrete Res*., **29**, 1491 (1999).
2. C. Y. Rha, J. W. Seong, C. E. Kim, S. K. Lee and W. K. Kim, *J. Math. Sci*., **34**, 4653 (1999).
3. C. Y. Rha, C. E. Kim, C. S. Lee, K. I. Kim and S. K. Lee, *Cement Concrete Res*., **29**, 231 (1999).
4. Y. Xie, Y. Liu and G. Long, *J. Wuhan Univ. Technol*., **23**, 303 (2008).
5. W. Xueguan, L. Dongxu, B. Qinghan, G. Ligun and T. Mingshu, *Cement Concrete Res*., **17**, 709 (1987).

6. A. Sari, C. Alkan, A. Karaipekli and A. Önal, *Energy Convers. Manage.*, **49**, 373 (2008).
7. T. Pompe, S. Zschoche, N. Herold, K. Salchert, M. F. Gouzy, C. Sperling and C. Werner, *Biomacromolecules*, **4**, 1072 (2003).
8. S. M. Henry and H. Liu, *Biomacromolecules*, **7**, 2407 (2006).
9. X. Yin and H. D. H. Stöver, *Macromolecules*, **36**, 8773 (2003).
10. C. Bunyakan and D. Hunkeler, *Polymer*, **40**, 6213 (1999).
11. C. Bunyakan, L. Armanet and D. Hunkeler, *Polymer*, **40**, 6225 (1999).
12. M. Wang, X. Zhu, S. Wang and L. Zhang, *Polymer*, **40**, 7387 (1999).
13. S. S. Hou and P. L. Kuo, *Polymer*, **42**, 2387 (2001).
14. C. Tang, S. Ye and H. Liu, *Polymer*, **48**, 4482 (2007).
15. J. E. Jönsson, H. Hassander and B. Törnell, *Macromolecules*, **27**, 1932 (1994).
16. T. M. Chou, P. Prayoonthong, A. Aitouchen and M. Libera, *Polymer*, **43**, 2085 (2002).
17. B. Lothenach, T Matschei, G. Möschner and F. P. Glasser, *Cement Concrete Res.*, **38**, 1 (2008).
18. X. Yin and H. D. H. Stöver, *Macromolecules*, **35**, 10178 (2002).
19. O. G. Atici, A. Akar and R. Rahimian, *Turk. J. Chem.*, **25**, 259 (2001).
20. N. Ogawa, K. Honmyo, K. Harada and A. Sugii, *J. Appl. Polym. Sci.*, **29**, 2851 (1984).
21. M. Sclavns, P. Franquinet, V. Carlier, G. Verfaille, I. Fallais, R. Legras, M. Laurent and F. C. Thyrion, *Polymer*, **41**, 1989 (2000).
22. P. K. Meth and P. J. Monteiro, Concrete: Microstructure, Properties, and Materials, 3rd Ed. McGraw-Hill, New York (2006).
23. Y. Lu and Jan D. Miller, *J. Colloid Interface Sci.*, **256**, 41 (2002).
24. C. M. Jugroot, T. G. M. van de Ven and M. A. Whitehead, *J. Phys. Chem. B.*, **109**, 7022 (2005).
25. I. Ogawa, H. Yamano and K. Miyagawa, *J. Appl. Polym. Sci.*, **47**, 217 (1993).
26. Y.-D. Luo, C.-A. Dai and W.-Y. Chiu, *J. Colloid Interface Sci.*, **330**, 170 (2009).
27. A. Li, J. Zhang and A. Wang, *Polym. Adv. Technol.*, **16**, 675 (2005).
28. J. Snuparek and V. Cermark, *Eur. Polym. J.*, **33**(8), 1345 (1997).
29. A. Li, A. Wang and J. Chen, *J. App. Polym. Sci.*, **94**, 1869 (2004).
30. S. Diamond, *Cement Concrete Res.*, **30**, 1517 (2000).